


# Human intrinsic choroidal neurons do not alter the expression of intrinsic markers in response to pressure

Christian Platzl,<sup>1</sup> Alexandra Kaser-Eichberger,<sup>1</sup> Heidi Wolfmeier,<sup>1</sup> Andrea Trost,<sup>2</sup> Falk Schroedl <sup>1</sup>

► Additional supplemental material is published online only. To view, please visit the journal online (<http://dx.doi.org/10.1136/bjophthalmol-2021-320211>).

<sup>1</sup>Center for Anatomy and Cell Biology, Institute of Anatomy and Cell Biology – Salzburg, Paracelsus Medical University, Salzburg, Austria

<sup>2</sup>University Clinic of Ophthalmology and Optometry, Research Program for Ophthalmology and Glaucoma Research, Paracelsus Medical University, Salzburg, Austria

## Correspondence to

Professor Falk Schroedl, Institute of Anatomy and Cell Biology-Salzburg, Paracelsus Medical University, Salzburg, Austria; [falk.schroedl@pmu.ac.at](mailto:falk.schroedl@pmu.ac.at)

CP and AK-E contributed equally.

Received 4 August 2021  
Accepted 30 November 2021  
Published Online First  
21 December 2021



© Author(s) (or their employer(s)) 2023. No commercial re-use. See rights and permissions. Published by BMJ.

**To cite:** Platzl C, Kaser-Eichberger A, Wolfmeier H, et al. *Br J Ophthalmol* 2023;**107**:1209–1215.

## ABSTRACT

**Background** The choroid is densely innervated by all parts of the autonomic nervous system and further harbours a network of local nerve cells, the intrinsic choroidal neurons (ICN). Their function in ocular control is currently unknown. While morphological data assume a role in intraocular pressure regulation, we here test if increased pressure on isolated choroids may activate ICN. **Methods** Donor tissue was transferred into a pressurisable tissue culture chamber, and nasal and temporal choroid halves incubated for 1 or 4 hours, with pressures set to 15 or 50 mm Hg, followed by qRT-PCR expression analysis of the ICN-specific markers VIP, UCN, NOS1, UCH-L1. POL2-normalised data in the different pressure settings, incubation times and localisations were statistically analysed.

**Results** The presence of the ICN-specific markers VIP, UCN, NOS1, UCH-L1 was confirmed using immunohistochemistry, and mRNA of all markers was detected in all experimental conditions. Marker analysis revealed no significant changes of mRNA expression levels between 15 and 50 mm Hg in the different incubation times. When comparing all samples over all experimental conditions, a significant increase of VIP and NOS1 mRNA was detected in temporal versus nasal choroids.

**Conclusion** In this functional analysis of human ICN *in vitro*, higher amounts of VIP and NOS1 mRNA were detected in the temporal choroid, that is, the choroidal site with ICN accumulation. Further, our data indicate that elevated pressure is apparently not able to trigger ICN responses via the investigated markers. Alternative markers and stimuli need to be investigated in upcoming studies in order to unravel ICN function.

## INTRODUCTION

The choroid, the middle layer of the eye, is one of the tissues with the highest blood flow rates in the human body.<sup>1</sup> This excessive blood flow is essential for the maintenance of adequate oxygen and nutrition supply of the retinal photoreceptors, and is therefore crucial for proper visual function. In order to adequately control this blood flow, the eye is densely innervated by the autonomic nervous system. Here, parasympathetic, sympathetic and also primary afferent (sensory) nerve fibres are involved in ocular and choroid control.<sup>2</sup>

A special feature in choroid innervation is the presence of nerve cells residing within the choroid, the intrinsic choroidal neurons (ICN). In humans,

they count for up to 2500 per eye forming a dense plexus, and it has been suggested that ICN serve as a local choroidal control mechanism. Although ICN have been described first some 150 years ago,<sup>3</sup> their function(s) is still unclear.<sup>4,5</sup> Morphological data suggest choroidal blood vessels as a target,<sup>6</sup> and this would allow for a local control of choroidal blood flow. Since ICN are also contacted by all parts of the cranial autonomic nervous system, and probably also contact each other,<sup>6,7</sup> they are somehow integrated within the autonomic regulation of the eye.<sup>8</sup> Again, the interdependency of all these sources regarding choroidal and ocular control is not understood.<sup>5</sup>

According to WHO reports, glaucoma is the second leading cause of blindness worldwide,<sup>9</sup> and high intraocular pressure (IOP) is one of the major risk factors.<sup>10,11</sup> This, however, cannot explain glaucoma(s) associated with normal IOP, and here dysregulation of ocular blood flow is one of the generally accepted causes.<sup>12</sup> Nowadays, pharmacological treatments in both cases involve drugs that directly act on or via the autonomic nervous system (eg,  $\beta$ -blockers,  $\alpha$ 2-adrenergic agonists, miotics, rho-kinase inhibitors)<sup>13,14</sup> in order to slow down disease progression, while a direct cure, despite available surgical interventions,<sup>15</sup> is still not available. Interestingly, in glaucomatous eyes with high IOP, the amount of ICN is drastically decreased,<sup>16</sup> although it is not known if this is a cause or reason of autonomic dysfunction. While also for age-related macular degeneration, the leading cause of blindness in elder people in the western hemisphere, a dysfunction of choroidal hemodynamics is discussed,<sup>17</sup> the need for a better understanding of choroidal nervous control and the role of ICN in this respect is obvious. If one assumes an involvement of ICN in the regulation of choroidal blood flow and IOP, then ICN should respond in some way to changes in these parameters. Therefore, and in order to better understand choroidal autonomic regulation, we investigated, for the very first time, the response of human ICN to elevated pressure in an *in vitro* approach, followed by analysis of expression profile of ICN-specific neurochemical markers.

## MATERIAL AND METHODS

In total, the choroids of 22 human donors (age 35–79 years, both sexes, postmortem time 9–24 hours) were analysed with no obvious ocular

**Table 1** Primary antibodies used in this study

Antigen	Gene name	Host	Dilution	Supplier (Cat #)
Vasoactive intestinal peptide	VIP	Guinea pig	1:1000	Progen, Heidelberg, Germany (16071)
Urocortin	UCN	Goat	1:400	Santa Cruz, Heidelberg, Germany (sc 1825)
Neuronal nitric oxide synthase	NOS1	Rabbit	1:100	Enzo Life Sciences, Lörrach, Germany (BML-SA227-0025)
Ubiquitin C-terminal hydrolase L1	UCH-L1	Guinea pig	1:400	Chemicon, Vienna, Austria (AB5898)

pathological alterations or acute chemotherapy. Since whole globes were obtained with intact vitreous/retina, temporal versus nasal choroid halves could be easily identified due to the position of the macula, prior to choroidal removal.

### Immunohistochemistry

In order to document adequate targets for expression analysis, immunohistochemistry was performed on choroidal flat-mount sections (three donors, both sexes, 35–73 years of age, post-mortem time 10–14 hours). The choroids were mounted in a cryostat (HM 550, Microm, Walldorf, Germany) and serial sections of 12–20 µm were collected on adhesion slides (Superfrost Plus; Thermo Scientific, Vienna, Austria), air-dried for at least 1 hour at room temperature (RT) and stored at –20°C for further processing. After a 5 min rinse in Tris-buffered saline (TBS; Roth, Karlsruhe, Germany) slides were incubated for 1 hour at RT in TBS containing 5% donkey serum (Sigma-Aldrich, Vienna, Austria), 1% bovine serum albumin (BSA; Sigma-Aldrich) and 0.5% Triton X-100 (Merck, Darmstadt, Germany). Following a 5 min rinse, slides were incubated for single and double immunolabelling with antibodies generated against VIP, urocortin (UCN), NOS1 and UCH-L1 (table 1, all diluted in TBS, containing 1% BSA and 0.5% Triton X-100, 12 hours at RT). After a rinse in TBS (three times for 5 min), the binding sites of primary antibodies were visualised by Alexa 555-tagged and/or Alexa 488-tagged antibodies (both 1:1000; raised in donkey; Invitrogen, Karlsruhe, Germany), in TBS containing 1% BSA and 0.5% Triton X-100 (1 hour at RT), followed by another rinse in TBS (three times for 5 min) and embedding in TBS–glycerol (1:1 at pH 8.6). Negative controls were performed by omission of the primary antibodies during incubation and revealed absence of immunoreactivity (controls). All antibodies used were generated against human epitopes and have been successfully applied in earlier studies. For documentation, a confocal laser scanning unit (Axio Observer Z1 attached to LSM710; ×20 dry or ×40 and ×60 oil immersion objective lenses, with numeric apertures 0.8, 1.30 and 1.4, respectively; Zeiss, Göttingen, Germany) was used. Sections were imaged using the appropriate filter settings for Alexa 555 (568 nm excitation, channel 1, coded red), Alexa 488 (488 nm excitation, channel 2, coded green) and DAPI (345 nm excitation, coded blue), and identical settings were used for the corresponding controls. For documentation of NOS1, a

fluorescence microscope was used (Axio Imager M2 equipped with AxioCam HRC and ApoTome 2 Unit; all Zeiss).

### Pressure treatment

Choroids were dissected in ice-cold Krebs-Ringer solution (NaCl 118 mM, NaHCO<sub>3</sub> 25 mM, Glucose 11.1 mM, KCl 4.7 5 mM, CaCl<sub>2</sub> 2.54 mM, MgSO<sub>4</sub> 1.2 mM, NaH<sub>2</sub>PO<sub>4</sub> 1 mM) and R retinal pigment epithelium was removed by gentle wiping with cotton swabs. Choroids were separated into temporal (site of high ICN concentration)<sup>18</sup> and nasal halves (site of low ICN concentration),<sup>18</sup> as identified by localisation of the retinal macula. Each half was transferred into a modified tissue culture chamber (Minucells, Bad Abbach, Germany),<sup>19</sup> equipped with a pressure transducer that allowed for continuous pressure recording in the mbar range (CPT2500, Wika, Vienna, Austria). The tubing of the chamber exit was adjustable in height and thereby enabled for different pressure settings. The tissue chamber was permanently rinsed with Krebs-Ringer solution (35 µL/min) using a four-channel peristaltic pump (Ismatec ISM597D, Cole-Parmer, Wertheim, Germany) and kept at 37°C using a heating plate, while the attached tubing system (Minucells) allowed for oxygen saturation via diffusion. Choroidal punches of 6 mm diameter were used for 1-hour incubations, while choroidal halves were chosen for the 4-hour experiments. Tissues were incubated free floating with chamber pressure set to 15 mm Hg (control) or chamber pressure set to 50 mm Hg (high pressure), respectively. A sketch of the experimental set-up is provided in online supplemental file 1

### Expression analysis

For expression analysis of neuronal markers expected to be expressed by activated ICN, choroids were snap frozen in liquid nitrogen immediately after pressure treatment and subsequently stored at –80°C until RNA isolation with the Roche High Pure RNA Tissue kit (Roche Molecular Systems; Vienna, Austria).

In brief, frozen tissue was transferred directly into 800 µL lysis buffer and homogenised using a TissueRuptor (Qiagen, Hilden, Germany). After a centrifugation step to remove tissue debris, 0.5 volumes of 96% ethanol were added to the supernatant and the suspension was loaded on a spin column.

**Table 2** Sequences of PCR primers for qPCR

Gene (refseq ID)	Forward primer (5'–3')	Reverse primer (5'–3')	Amplicon size (bp)
VIP (NM_003381.4, NM_194435.3)	TGAATGGAAAGAGGAGCAGTGAGG	CACTGGGAAGTTGTCATCAGCTTTG	105
NOS1 (NM_000620.5, NM_001204218.1, NM_001204214.1, NM_001204213.1)	ATGCTGCTAATCTCTGCCAAGT	CAACCTCGCAAAGAGCGTG	85
UCHL1 (NM_004181.4)	CCTGTGGCACAATCGGACTT	TACCCGACATTGGCCTTCT	197
UCN (NM_003353.4)	CCGAGCAGAACCGCATCATA	AGGGGTCAACGTTTTTCGCAG	76
POL2 (NM_000937.5)	GAAGCTGGTGCTCCGTATT	CAGGAAGACATCATCCATCT	97
HPRT1 (NM_000194.3)	TTCTTGGTCAGGCAGTATAATC	GGGCATATCTACAACAACCTTG	137

**Table 3** Samples and analysis of the experimental conditions with 1-hour incubation time

Target	Side	Treatment time (h)	15 mm Hg sample size	Relative expression mean 15 mm Hg	Relative expression median 15 mm Hg	50 mm Hg sample size	Relative expression mean 50 mm Hg	Relative expression median 50 mm Hg	P value (statistical test)	Fold induction
VIP	T	1	20	0.063	0.074	20	0.052	0.044	0.398 (Wilcoxon)	-1.2
UCN	T	1	20	0.014	0.011	20	0.013	0.010	0.820 (Wilcoxon)	-1.1
NOS1	T	1	16	0.021	0.027	14	0.023	0.023	0.951 (Wilcoxon)	1.1
UCH-L1	T	1	14	0.194	0.332	13	0.368	0.569	0.259 (Wilcoxon)	1.9
VIP	N	1	20	0.029	0.025	20	0.038	0.032	0.495 (Wilcoxon)	1.3
UCN	N	1	20	0.013	0.011	20	0.012	0.011	0.678 (Wilcoxon)	-1.1
NOS1	N	1	18	0.007	0.007	16	0.009	0.010	0.384 (Wilcoxon)	1.3
UCH-L1	N	1	16	0.245	0.294	15	0.227	0.232	0.682 (Wilcoxon)	-1.1

N, nasal side; T, temporal side.

Following DNase digestion, washing steps were performed according to the manufacturer's instructions (Roche Molecular Systems; Vienna, Austria). Total RNA was eluted in elution buffer, and RNA concentration was determined with a low volume photometer (Nanophotometer P300, Implen, Munich, Germany). Up to 0.5 µg of eluted total RNA were used for cDNA synthesis (iScript cDNA synthesis kit; BioRad, Vienna, Austria), and quantitative PCR (qPCR) was performed with GoTaq qPCR Master Mix (Promega; Madison, Wisconsin, USA). Primers for amplification of neuronal marker genes (VIP, NOS1, UCHL1, UCN) and housekeeping gene (POL2, HPRT) are listed in table 2. In all samples, HPRT1 and POL2 have been used as reference genes. Since the POL2 revealed a more robust expression (ie, CT detectable below 32 cycles even in low template RNA) compared with HPRT1, therefore the prior one was used as reference gene. Primers have been designed using the NCBI Primer design tool, whenever applicable, primers were designed to amplify all transcription variants according to the RefSeq Database (VIP and NOS1). Primer specificity was proven by melt curve control, size estimation by agarose gel electrophoresis (4% Biozym Sieve 3:1 Agarose; Biozym, Vienna, Austria) and sequencing of the PCR products. Each reaction was run in duplicates on a CFX96 Thermal Cycler (C1000 Thermal Cycler; BioRad, Vienna, Austria) with a three-step protocol (3' initial denaturation 95°C, 40 cycles: 10' 95°C, 20' 60°C, 20' 72°C). No template controls were included in the analysis.

PCR data from analysed genes were normalised to the RNA of POL2 to calculate a relative expression value defined as  $2^{-(C_{\text{target gene}} - C_{\text{reference gene}})}$ . The relative expression levels from controls (15 mm Hg) were compared with relative expression levels from high-pressure-treated choroids (50 mm Hg).

Data from all experiments (including all outliers) were statistically analysed with the analysis software R (The R Foundation, www.r-project.org), and graphically displayed as box plots. Whenever possible, a Student's t-test was applied to calculate a p value (with p values < 0.05 considered as statistically significant), otherwise a Wilcoxon rank-sum test was used (based on a preceding Shapiro-Wilk test for normal distribution). Data of all experimental conditions and samples analysed are summarised in table 3 (1-hour incubation) and table 4 (4-hour incubation).

## RESULTS

### Immunohistochemistry

When applying immunohistochemistry for the neuroregulatory peptides VIP and UCN, and the enzymes NOS1 and UCH-L1, these markers were detectable in ICN, but not in other structures of the choroid, and since extrinsic sources from autonomic cranial ganglia are removed due to the preparation technique, the mentioned markers are considered ICN specific. While both VIP and UCN revealed a fine granular pattern within the cytosol of ICN, with VIP being more distinctive, the enzymes NOS1 and UCH-L1 displayed a more prominent cytosolic immunoreactivity, and were also detectable in processes emerging from ICN (figure 1). All negative controls displayed absence of immunoreactivity (figure 1).

### Expression analysis

The ICN-specific mRNA's for VIP, UCN, NOS1 and UCH-L1 were detectable in all specimens and all experimental conditions investigated. At least 13 different samples per condition have been analysed (see table 3 for samples in the

**Table 4** Samples and analysis of the experimental conditions with 4-hour incubation time

Target	Side	Treatment time (h)	15 mm Hg sample size	Relative expression mean 15 mm Hg	Relative expression median 15 mm Hg	50 mm Hg sample size	Relative expression mean 50 mm Hg	Relative expression median 50 mm Hg	P value (statistical test)	Fold induction
VIP	T	4	9	0.011	0.006	9	0.015	0.015	0.605 (Wilcoxon)	1.4
UCN	T	4	9	0.009	0.011	9	0.009	0.008	0.974 (t-test)	1.0
NOS1	T	4	9	0.009	0.007	9	0.011	0.009	0.931 (Wilcoxon)	1.2
UCH-L1	T	4	9	0.283	0.233	9	0.299	0.241	0.730 (Wilcoxon)	1.1
VIP	N	4	8	0.011	0.013	8	0.011	0.013	0.959 (Wilcoxon)	1.0
UCN	N	4	8	0.009	0.009	8	0.009	0.010	0.721 (Wilcoxon)	1.0
NOS1	N	4	8	0.006	0.006	8	0.007	0.006	0.959 (Wilcoxon)	1.2
UCH-L1	N	4	8	0.235	0.255	7	0.198	0.201	0.779 (Wilcoxon)	-1.2

N, nasal side; T, temporal side.

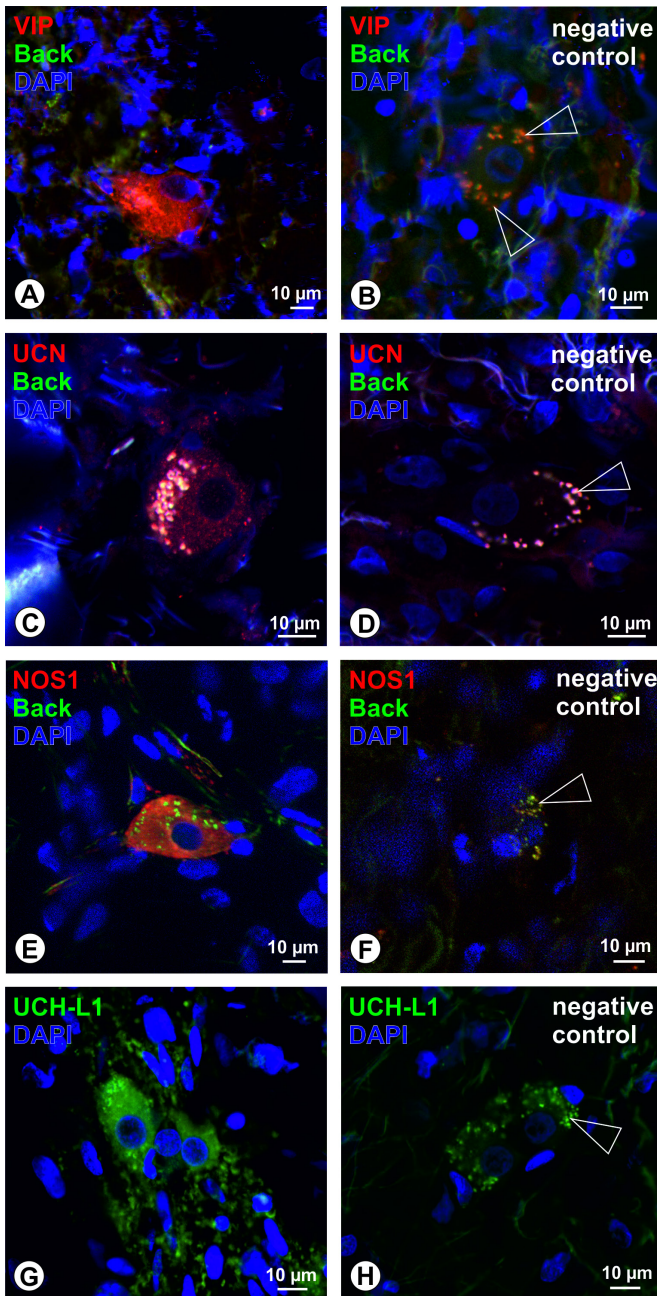


**Figure 1** Immunohistochemistry detected the neuroregulatory peptides VIP (red, A) and UCN (red, C) with fine granular pattern within the soma of intrinsic choroidal neurons (ICN), while corresponding negative controls revealed absence of immunoreactivity (B,D). Further, immunoreactivity for the ICN-specific enzymes NOS1 (E, red) and UCH-L1 (G, green) was detected with clear somatic distribution. Again, immunoreactivity was absent in corresponding negative controls (F,G). Note, the accumulation of autofluorescent lipofuscin-granules in all micrographs (marked with arrowheads in the negative controls; Back=background; blue=nuclear DAPI staining), that allowed for unequivocal identification of ICN in the negative controls (A–D, and G,H represent confocal images in single optical section mode. E,F represent optical sections of the fluorescence microscope).

various conditions). Following a 1-hour incubation of the temporal halves in normal compared with high-pressure settings (figure 2), no significant changes in the mRNA content were observed (normalised to POL2, p values for:

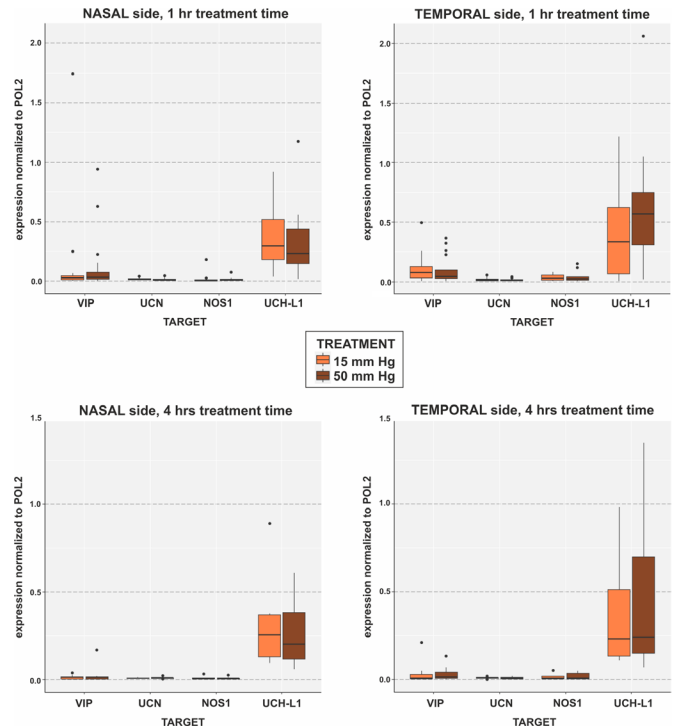


**Figure 2** Box plots of expression analysis of samples analysed in the different experimental conditions (15 vs 50 mm Hg; 1-hour treatment vs 4-hour treatment), normalised to the housekeeping gene POL2. Outliers are indicated (black dots). A statistical significance in the different experimental conditions was not detected.

VIP=0.398; UCN=0.82; NOS1=0.951; UCH-L1: 0.259). When comparing the data obtained from nasal halves in identical conditions, again no statistical significance was reached (p values for: VIP=0.495, UCN=0.678; NOS1=0.384; UCH-L1=0.682).

Since a 1-hour pressurisation did not result in detectable changes in the investigated RNA content, an alternative setting with an incubation time of 4 hours was chosen (see figure 2). At least seven different samples per experimental condition have been analysed (see table 4 for samples in the various conditions). Again, temporal halves revealed no statistical significance when comparing the POL2-normalised mRNA content in normal-pressure versus high-pressure choroids (p values for: VIP=0.605, UCN=0.974; NOS1=0.931; UCH-L1: 0.730). Also, analysis of the nasal halves revealed no statistically significant changes (p values for: VIP=0.959; UCN=0.721; NOS1=0.959; UCH-L1=0.779).

When analysing the outliers separately in the different experimental conditions (see figures 2 and 3), a relation between high donor age or prolonged postmortem time was not detected.

When the temporal versus nasal halves were compared over all experimental conditions (see figure 3, and table 5), however, a statistical significance in the content of VIP and NOS1 was reached (VIP=0.043; NOS1=0.001).

Analysis of the experimental duration compared over all experimental conditions (1 vs 4 hours; figure 4, table 6) revealed a significant reduction of VIP and UCN (p=0.000 and p=0.009, respectively), while NOS1 and UCH-L1 remained unaltered.

## DISCUSSION

In order to meet with the retinal demands, the choroid processes multiple extrinsic and intrinsic signals to provide proper regulation.<sup>20</sup>

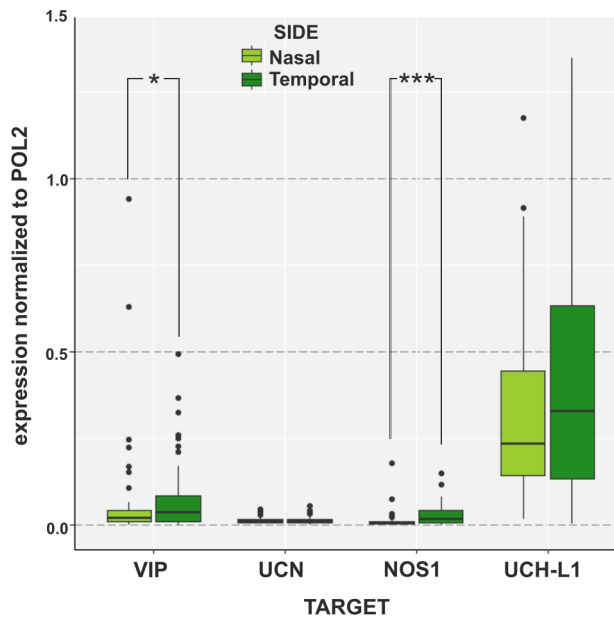


**Figure 3** Box plots of expression analysis of all temporal versus nasal samples analysed over all experimental conditions (15 and 50 mm Hg; 1-hour treatment and 4-hour treatment), normalised to the housekeeping gene POL2. Outliers are indicated (black dots). Over the different experimental conditions, a statistical significance was reached for VIP (p=0.043) and NOS1 (p=0.001) when comparing temporal versus nasal halves.

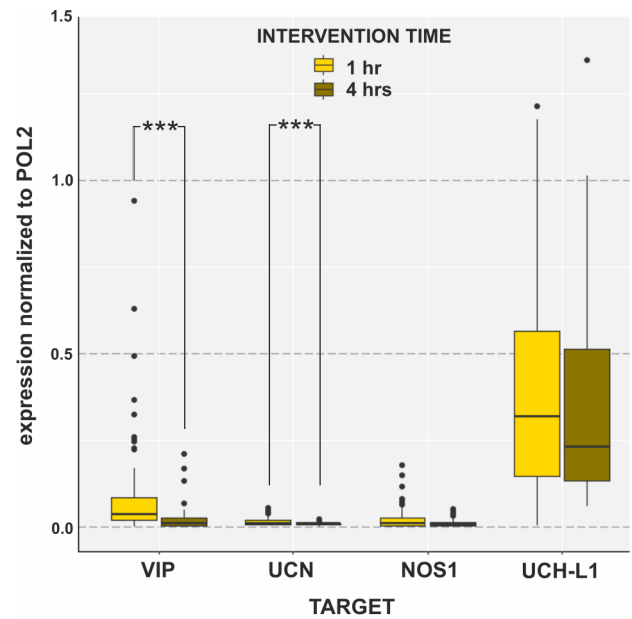


**Figure 4** Box plots of expression analysis of all 1-hour treatment and 4-hour treatment samples over all experimental conditions (15 and 50 mm Hg; temporal and nasal), normalised to the housekeeping gene POL2. Outliers are indicated (black dots). Over the different experimental conditions, a statistical significance was reached for VIP (p=0.000) and UCN (p=0.009) when comparing 1-hour-treated samples versus 4-hour-treated samples.

While some humoral factors of the retinochoroidal axis have been described,<sup>21</sup> the exact interplay is not understood. This holds also true with respect to the autonomic nervous system: while extrinsic sources are known (sympathetic, parasympathetic, primary afferent), the function of the intrinsic source (ICN) is not known, and it seems that ICN exhibit various regulatory functions with yet unknown triggers.<sup>2,22</sup> So far, morphological data only indicate an involvement of ICN in the regulation of choroidal blood flow, subsequently affecting IOP<sup>5</sup>: ICN contain and release the neurotransmitter nitric oxide (NO), suggesting a relaxation of choroidal blood vessels,<sup>23</sup> followed by an increase in choroidal blood flow. This, in turn, would potentially lead to an alteration in IOP, since these parameters are somehow related.<sup>24,25</sup> The same holds true for the other markers investigated (VIP, UCN), leading to vasodilation/smooth muscle relaxation.<sup>26,27</sup> Here, we investigated if elevated pressure is a trigger for human ICN to change the expression profile of selected ICN markers.

Based on preceding (morphological) data, pressure has been hypothesised to be an adequate stimulus in choroidal intrinsic control.<sup>6</sup> Therefore, in this setting, the physiological IOP situation (15 mm Hg)<sup>28</sup> was compared with a high-pressure situation (50 mm Hg) that can be reached or even exceeded in closed angle glaucoma.<sup>29</sup> In human glaucomatous eyes,<sup>16</sup> a loss of ICN has been reported,

hinting towards a connection between high IOP and damaged ICN. A monkey model of experimentally induced high IOP, however, revealed constant ICN numbers after 4 weeks.<sup>30</sup> While this might argue for a more chronic effect onto ICN, we therefore do not anticipate ICN damage due to 4 hours of high-pressure treatment, as used in our model. Additionally, earlier experiments with human choroids demonstrated that the intrinsic network is vital up to 2 days within the in vitro environment chosen,<sup>6</sup> and therefore seems suitable for our stimulation. While the potential mechanism of ICN action related to pressure changes is not clear, ICN could act as a sensor per se (via pressure sensitive channels), via tissue stretch/strain (as evidenced by close contacts to non-vascular smooth muscle cells<sup>6,8</sup>) or via the filling state of choroidal blood vessels. These are, at least in the animal model, also connected to the non-vascular smooth muscle framework of the choroid.<sup>31</sup> Any of the afore-mentioned features, alone or in combination, would therefore allow for the detection of alterations in the choroidal ‘sponge’ under normal versus high pressure. It is also clear that the here provided pressure stimulus is not able to fully reflect true IOP situations for obvious reasons, but rather represents a pressure related experimental approach in the isolated choroid.

**Table 5** Analysis of temporal versus nasal choroidal halves over all experimental conditions

Target	Pressure	Treatment time (h)	Nasal sample size	Relative expression mean nasal	Relative expression median nasal	Temporal sample size	Relative expression mean temporal	Relative expression median temporal	P value (statistical test)	Fold induction
VIP	15 and 50	1 and 4	56	0.024	0.021	58	0.036	0.038	0.043* (Wilcoxon)	1.5
UCN	15 and 50	1 and 4	56	0.011	0.010	58	0.012	0.011	0.685 (Wilcoxon)	1.1
NOS1	15 and 50	1 and 4	50	0.007	0.008	48	0.016	0.018	0.001* (Wilcoxon)	2.3
UCH-L1	15 and 50	1 and 4	46	0.230	0.236	45	0.275	0.346	0.172 (Wilcoxon)	1.2

As readout, the mRNA expression levels of ICN-specific 'regulators' have been chosen, and the in vitro approach is advantageous in that all extrinsic autonomic innervation is removed that otherwise potentially could influence results obtained with intact extrinsic innervations (ie, it is not known which system influences/overwrites another system and to which extent). Further, it is also widely known that parasympathetic nerve fibres also contain both NO and VIP, thus making a discrimination difficult. While ICN express a panel of multiple neuroregulatory peptides,<sup>7 8 32 33</sup> the 'main action' is currently discussed via their content of NO (see above) and VIP. These neurotransmitters/neuropeptides are expressed in the vast majority of ICN, and therefore have been included for analysis in the current study, thus increasing the chance to detect an alteration in this experimental design.

Analysing the expression of NOS1 and VIP in the two halves (nasal vs temporal) over all samples and all conditions revealed that the ICN exclusive markers were significantly increased in the temporal part. This fits well with the topographical organisation of ICN: being more concentrated in temporal than nasal parts of the choroid.<sup>18</sup> The reason for this topographical difference is not clear. It could be speculated that a more pronounced regulation in areas with high visual acuity seems necessary and provides the reason for such a topographical difference, while apparently the macula region itself lacks considerable amounts of ICN.<sup>34</sup> Regarding VIP, a significant decrease was observed when comparing 1-hour versus 4-hour incubation time. While this could argue for the loss of extrinsic regulation in the isolated choroid, the mechanisms behind this are unclear, and many other unknown factors could contribute here.

In this context, analysis of UCN never reached significance in the different pressure conditions. Although vasodilatory effects of UCN are well known,<sup>35</sup> and are therefore concomitant with NOS1 and VIP effects, we interpret our UCN results as an ancillary impact for pressure related aspects, which are maybe more related to modulatory effects in neurotransmission. Regarding analysis over time, a statistical significant decrease in UCN expression (1 vs 4 hours) was detected. This decrease was smaller than the decrease of VIP. However, since the housekeeping genes POL2/HPRT1 and also UCHL-1 (see below) remained unaltered, this indicates an intact tissue after 4-hour incubation. One could therefore speculate that some unknown missing choroidal input/stimulation is responsible for the observed decrease in VIP and UCN.

Interesting in this sense is the behaviour of UCHL-1. While it represents an enzyme that acts as both ligase and hydrolase, it is of high importance for protein recycling and degradation,<sup>36</sup> and is expressed in almost all neuronal cells of the central and peripheral nervous system, for which it serves as a pan-neuronal marker.<sup>37</sup> While it serves also as a prognostic marker in various tumours,<sup>38</sup> UCHL-1 is also altered in various acute CNS injuries.<sup>39</sup> In our experimental

setup, we would therefore anticipate increased UCHL-1 levels in the high-pressure environment as a result of increased neuronal reaction/turn over. Regarding our data, this was not the case, arguing against pressure as an appropriate trigger for ICN action. Nevertheless, it could argue for our setup (and read out) not harming ICN after 4-hour incubation, and is also supported by our data of intervention time where significant changes between 1 and 4 hours were not observed. While in other experiments, significantly increased UCHL-1 mRNA levels were observed in murine podocytes when stimulated with TNF $\alpha$  even after 1-hour incubation,<sup>40</sup> this holds also true for NOS1 mRNA levels that were elevated following 1-hour and 4-hour pharmacological stimulation in a brain slice model.<sup>41</sup>

mRNA analysis for our set-up was chosen since from our understanding this represents a feasible and most robust read-out possibility for the chosen target (ICN). We anticipated a direct response on pressure stimulation, not dealing with pitfalls in peptide degradation and detection limits (eg, VIP, GAL) or pitfalls in direct NO measurement (NOS1 vs NOS3). Another technical issue was solved during the experimental process: in early experimental stages, dermal biopsy punches of 6 mm diameter were used to better standardise tissue harvest. When processing these punches, obtained RNA content was detectable but low, and we therefore decided to use choroid halves instead in the 4-hour experiments (but however, included those biopsy samples in the total sample analysis; tables 3, 5 and 6). Since 1-hour experiments showed no significant changes in the investigated mRNA content, the 4-hour experiments were carried out to confirm these findings and to investigate a possible prolonged pressure time necessary for putative reaction of the intrinsic system to these changes.

Taken together, our data could prove a difference in temporal versus nasal halves of the choroid that matches with the topographical distribution of human ICN. In this respect, a difference in ICN distribution in the avian animal model should be considered.<sup>42</sup> While here pressure seems apparently not crucial for ICN activation, initial reaction(s) to IOP might happen also in the retina and retinal signals might be transduced to the choroid and ICN as a downstream effect, as for example, reported for increased choroidal blood flow after retinal light exposition.<sup>5 43</sup> If this is indeed the case, much longer transduction periods than expected would apply, but at the same time this consideration seems somehow questionable, given the anticipated immediate neuronal response on a given stimulus. On the other hand, our data might indicate that ICN action is rather involved in regulation of choroidal blood flow with its remarkable high flow rate<sup>1</sup> in order to protect the retina from thermal damage<sup>20</sup> or in the adjustment/equilibration of mechanical forces transferred into the choroid during accommodation.<sup>4</sup> The latter one would result in a more pronounced stretch response than the here provided pressure stimulus, and will be clarified in upcoming studies.

**Table 6** Analysis of 1-hour experiments versus 4-hour experiments over all experimental conditions

Target	Side	Pressure	1-hour sample size	Relative expression mean 1 hour	Relative expression median 1 hour	4-hour sample size	Relative expression mean 4 hours	Relative expression median 4 hours	P value (statistical test)	Fold induction
VIP	T and N	15 and 50	80	0.044	0.037	34	0.012	0.012	0.000* (Wilcoxon)	-3.7
UCN	T and N	15 and 50	80	0.013	0.011	34	0.009	0.01	0.009* (Wilcoxon)	-1.4
NOS1	T and N	15 and 50	64	0.013	0.012	34	0.008	0.007	0.075 (Wilcoxon)	-1.6
UCHL-1	T and N	15 and 50	58	0.249	0.325	33	0.255	0.233	0.533 (Wilcoxon)	1.0

N, nasal side; T, temporal side.

Since some data were not normal distributed after analysis with the Shapiro-Wilk test, the Wilcoxon-signed-rank test was applied. As this statistical test is not as sensitive as the Student's t-test, therefore slight differences between tested groups might not be detected, which is a limitation of this analysis.

Our study nevertheless represents the first functional analysis of human ICN action. It proved suitable to test for ICN triggers and function(s). Future pharmacological stimulation will shed more light on the still enigmatic ICN, in order to better understand choroidal mechanisms important for ocular homeostasis.

**Correction notice** Since this article was first published, the funding statement has been updated.

**Contributors** CP, AK-E, HW, AT and FS (guarantor): Contributed substantial to the conception and design of the work; the acquisition, analysis and interpretation of data for the work; drafting the work and revising it critically for important intellectual content; gave final approval of the work to be published; agreed to be accountable for all aspects of the work in ensuring that questions related to the accuracy or integrity of any part of the work are appropriately investigated and resolved. CP and AK-E contributed equally to this paper.

**Funding** Austrian National Bank Anniversary Fund (17617) and Research Fund of Paracelsus Medical University (PMU-FFF A-18/01/030- SCK).

**Competing interests** None declared.

**Patient consent for publication** Not applicable.

**Ethics approval** Human choroids were obtained from the Cornea Bank of the University Clinic of Ophthalmology and Optometry, or the body donor programme of the Center for Anatomy and Cell Biology, Institute of Anatomy and Cell Biology—Salzburg, both Paracelsus Medical University Salzburg, Austria, in full accordance with the Declaration of Helsinki and approved by the local ethics committee (415-EP/73/775-2018 and EK1012/2019).

**Provenance and peer review** Not commissioned; externally peer reviewed.

**Data availability statement** No data are available. Not applicable.

**Supplemental material** This content has been supplied by the author(s). It has not been vetted by BMJ Publishing Group Limited (BMJ) and may not have been peer-reviewed. Any opinions or recommendations discussed are solely those of the author(s) and are not endorsed by BMJ. BMJ disclaims all liability and responsibility arising from any reliance placed on the content. Where the content includes any translated material, BMJ does not warrant the accuracy and reliability of the translations (including but not limited to local regulations, clinical guidelines, terminology, drug names and drug dosages), and is not responsible for any error and/or omissions arising from translation and adaptation or otherwise.

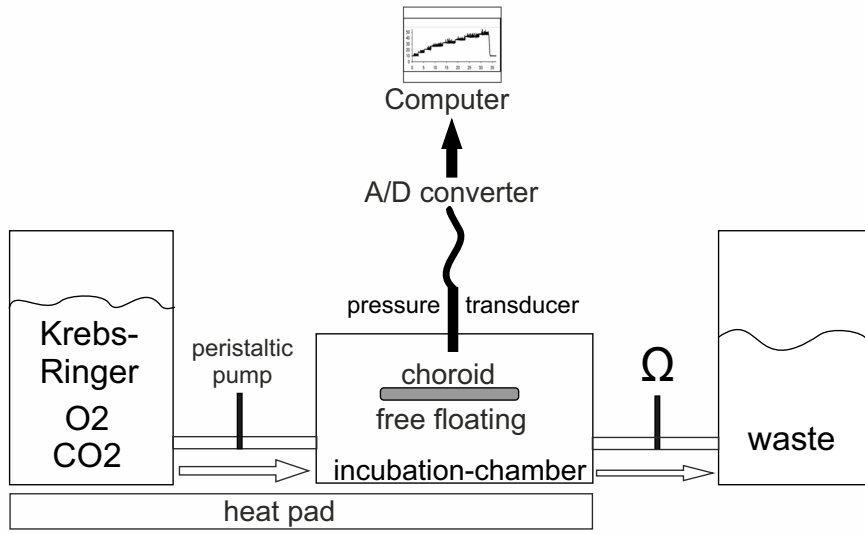
#### ORCID iD

Falk Schroedl <http://orcid.org/0000-0002-8807-8982>

#### REFERENCES

- Alm A, Bill A. Ocular and optic nerve blood flow at normal and increased intraocular pressures in monkeys (*Macaca irus*): a study with radioactively labelled microspheres including flow determinations in brain and some other tissues. *Exp Eye Res* 1973;15:15–29.
- McDougal DH, Gamlin PD. Autonomic control of the eye. *Compr Physiol* 2015;5:439–73.
- Müller H. Ueber glatte Muskeln und Nervengeflechte Der Chorioidea Im menschlichen Auge. *Verh physik-med Ges Würzburg* 1859;10:179–92.
- Schrodl F. Intrinsic choroidal neurons. In: Troger J, Kieselbach G, Bechrakis N, eds. *Neuropeptides in the eye*. Trivandrum: Research Signpost, 2009: 169–97.
- Reiner A, Fitzgerald MEC, Del Mar N, et al. Neural control of choroidal blood flow. *Prog Retin Eye Res* 2018;64:96–130.
- Schrodl F, De Laet A, Tassignon M-J, et al. Intrinsic choroidal neurons in the human eye: projections, targets, and basic electrophysiological data. *Invest Ophthalmol Vis Sci* 2003;44:3705–12.
- May CA, Neuhuber W, Lütjen-Drecoll E. Immunohistochemical classification and functional morphology of human choroidal ganglion cells. *Invest Ophthalmol Vis Sci* 2004;45:361–7.
- Stübinger K, Brehmer A, Neuhuber WL, et al. Intrinsic choroidal neurons in the chicken eye: chemical coding and synaptic input. *Histochem Cell Biol* 2010;134:145–57.
- Kingman S. Glaucoma is second leading cause of blindness globally. *Bull World Health Organ* 2004;82:887–8.
- McMonnies CW. Glaucoma history and risk factors. *J Optom* 2017;10:71–8.
- Enders P, Schaub F, Adler W, et al. The use of Bruch's membrane opening-based optical coherence tomography of the optic nerve head for glaucoma detection in microdiscs. *Br J Ophthalmol* 2017;101:530–5.
- Flammer J, Orgül S, Costa VP, et al. The impact of ocular blood flow in glaucoma. *Prog Retin Eye Res* 2002;21:359–93.
- Nocentini A, Supuran CT. Adrenergic agonists and antagonists as antiglaucoma agents: a literature and patent review (2013-2019). *Expert Opin Ther Pat* 2019;29:805–15.
- Shalaby WS, Shankar V, Razeghinejad R, et al. Current and new pharmacotherapeutic approaches for glaucoma. *Expert Opin Pharmacother* 2020;21:2027–40.
- Heindl LM, Siebelmann S, Dietlein T, et al. Future prospects: assessment of intraoperative optical coherence tomography in ab interno glaucoma surgery. *Curr Eye Res* 2015;40:1288–91.
- May CA, Lütjen-Drecoll E. Choroidal ganglion cell changes in human glaucomatous eyes. *J Glaucoma* 2004;13:389–95.
- van Lookeren Campagne M, LeCouter J, Yaspan BL, et al. Mechanisms of age-related macular degeneration and therapeutic opportunities. *J Pathol* 2014;232:151–64.
- Flügel C, Tamm ER, Mayer B, et al. Species differences in choroidal vasodilative innervation: evidence for specific intrinsic nitergic and VIP-positive neurons in the human eye. *Invest Ophthalmol Vis Sci* 1994;35:592–9.
- Minuth WW, Denk L. Supportive development of functional tissues for biomedical research using the MINUSHEET® perfusion system. *Clin Transl Med* 2012;1:22.
- Nickla DL, Wallman J. The multifunctional choroid. *Prog Retin Eye Res* 2010;29:144–68.
- Troilo D, Smith EL, Nickla DL, et al. IMI - Report on Experimental Models of Emmetropization and Myopia. *Invest Ophthalmol Vis Sci* 2019;60:M31–88.
- Neuhuber W, Schrödl F. Autonomic control of the eye and the iris. *Auton Neurosci* 2011;165:67–79.
- Troger J, Kieselbach G, Teuchner B, et al. Peptidergic nerves in the eye, their source and potential pathophysiological relevance. *Brain Res Rev* 2007;53:39–62.
- Bucolo C, Salomone S, Drago F, et al. Pharmacological management of ocular hypertension: current approaches and future prospective. *Curr Opin Pharmacol* 2013;13:50–5.
- Schmetterer L, Polak K. Role of nitric oxide in the control of ocular blood flow. *Prog Retin Eye Res* 2001;20:823–47.
- Onoue S, Misaka S, Yamada S. Structure-activity relationship of vasoactive intestinal peptide (VIP): potent agonists and potential clinical applications. *Naunyn-Schmiedeberg's Arch Pharmacol* 2008;377:579–90.
- Kageyama K, Teui K, Tamasawa N, et al. Regulation and roles of urocortins in the vascular system. *Int J Endocrinol* 2012;2012:1–6.
- Dietze J, Blair K, Havens SJ. *Glaucoma. StatPearls*. Treasure Island (FL), 2021.
- Dayan M, Turner B, McGhee C. Acute angle closure glaucoma masquerading as systemic illness. *BMJ* 1996;313:413–5.
- Albrecht May C, Kaufman PL, Lütjen-Drecoll E, et al. Choroidal innervation and optic neuropathy in macaque monkeys with laser- or anterior chamber perfusion-induced short-term elevation of intraocular pressure. *Exp Eye Res* 2006;82:1060–7.
- De Stefano ME, Mugnaini E. Fine structure of the choroidal coat of the avian eye. vascularization, supporting tissue and innervation. *Anat Embryol* 1997;195:393–418.
- de Hoz R, Ramírez AI, Salazar JJ, et al. Substance P and calcitonin gene-related peptide intrinsic choroidal neurons in human choroidal whole-mounts. *Histol Histopathol* 2008;23:1249–58.
- Kaser-Eichberger A, Trost A, Strohmaier C, et al. Distribution of the neuro-regulatory peptide galanin in the human eye. *Neuropeptides* 2017;64:85–93.
- Triviño A, De Hoz R, Salazar JJ, et al. Distribution and organization of the nerve fiber and ganglion cells of the human choroid. *Anat Embryol* 2002;205:417–30.
- Rademaker MT, Richards AM. Urocortins: actions in health and heart failure. *Clin Chim Acta* 2017;474:76–87.
- Matuszczak E, Tylicka M, Komarowska MD, et al. Ubiquitin carboxy-terminal hydrolase L1 - physiology and pathology. *Cell Biochem Funct* 2020;38:533–40.
- Barrenschee M, Böttner M, Harde J, et al. SNAP-25 is abundantly expressed in enteric neuronal networks and upregulated by the neurotrophic factor GDNF. *Histochem Cell Biol* 2015;143:611–23.
- Rong C, Zhou R, Wan S, et al. Ubiquitin carboxyl-terminal hydrolases and human malignancies: the novel prognostic and therapeutic implications for head and neck cancer. *Front Oncol* 2020;10:592501.
- Wang KK, Yang Z, Sarkis G, et al. Ubiquitin C-terminal hydrolase-L1 (UCH-L1) as a therapeutic and diagnostic target in neurodegeneration, neurotrauma and neuro-injuries. *Expert Opin Ther Targets* 2017;21:627–38.
- Zhang H, Sun Y, Hu R, et al. The regulation of the UCH-L1 gene by transcription factor NF-κB in podocytes. *Cell Signal* 2013;25:1574–85.
- Grange-Messent V, Raison D, Dugas B, et al. Noradrenaline up-regulates the neuronal and the inducible nitric oxide synthase isoforms in magnocellular neurons of rat brain slices. *J Neurosci Res* 2004;78:683–90.
- Schroedl F, De Stefano ME, Reese S, et al. Comparative anatomy of nitergic intrinsic choroidal neurons (ICN) in various avian species. *Exp Eye Res* 2004;78:187–96.
- Shih YF, Lin SY, Huang JK, et al. The choroidal blood flow response after flicker stimulation in chicks. *J Ocul Pharmacol Ther* 1997;13:213–8.

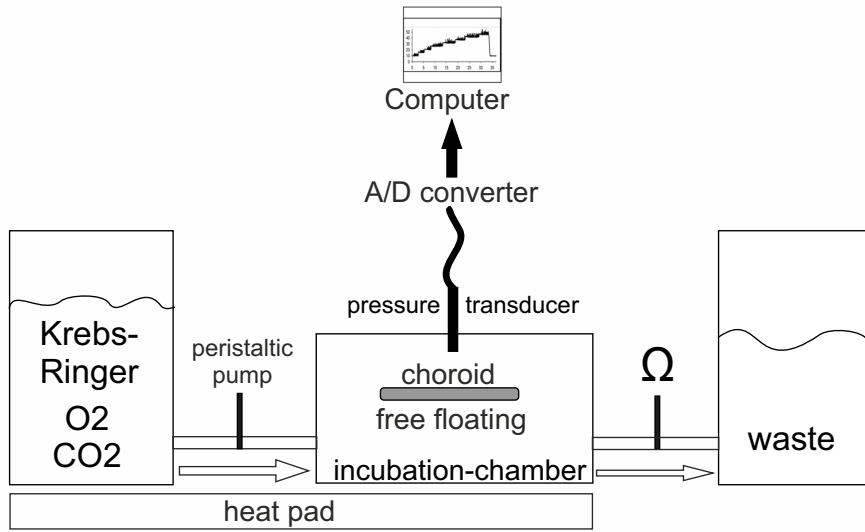
## Sketch of the experimental set-up



Suppl. 1



## Sketch of the experimental set-up



Suppl. 1